

Article

In Vitro Investigation of Antiaging Efficacy of Pterostilbene as Cosmetic Ingredient

Zongxiao Cen¹, Zhiyuan Chen¹, Ding Wang¹, Yuqin Zuo¹, Xueping Chen^{2,3,*}  and Junyuan Chen³

¹ Guangzhou Luanying Cosmetics Co., Ltd., 2210, 22nd Floor, No. 180, Jiangnan Road, Haizhu District, Guangzhou 510220, China

² Centre for Biotech Big Data Research & Development, Research Institute of Tsinghua, Pearl River Delta, Huangpu District, Guangzhou 510000, China

³ Vitargent (International) Biotechnology Limited, Unit 516, 5/F. Biotech Centre 2, No. 11 Science Park West Avenue, Hong Kong Science Park, Shatin, Hong Kong SAR, China

* Correspondence: xueping.chen@vitargent.com

Abstract: Pterostilbene is gaining increasing attention as an effective ingredient in cosmetics. This study was performed to investigate the antiaging efficacy of pterostilbene using a human-originated P2 generation fibroblast assay and an in vitro skin experiment. A fibroblast cytotoxicity assay was performed to evaluate the safety of pterostilbene: a 30 J/cm² UVA irradiated fibroblast cell assay and a 30 J/cm² UVA and 50 mJ/cm² UVB-irradiated in vitro skin experiment were carried out to evaluate the antiaging efficacy of pterostilbene. The cytotoxicity assay found that 3.90 µg/mL or lower concentrations of pterostilbene exerted no significant toxicity to fibroblasts. The fibroblast cell assay showed that 2.6 µg/mL pterostilbene alleviated the UVA damage to fibroblasts by down-regulating the gene expression of *matrix metalloproteinase 1 (MMP-1)* by 18.62% and decreasing the content of MMP-1 by 10.08%, MMP-3 by 15.10%, and collagen I by 33.92%. The in vitro skin experiment revealed that pterostilbene relieved the adverse UVA and UVB irradiation effects on skin tissue by increasing the thickness of the epidermis to maintain skin morphology, preventing the degradation of collagen fibers by 88.57%, and increasing the amount of collagen IV by 30.95%, collagen VII by 25.64%, and fibroblast growth factor-β (FGF-β) by 15.67%. This fibroblast assay and in vitro skin study consistently demonstrated the strong antiaging efficacy of pterostilbene.

Keywords: pterostilbene; fibroblast; *in vitro* skin; antiaging



Academic Editors:

Agnieszka Feliczak-Guzik and

Agata Wawrzyńczyk

Received: 25 November 2024

Revised: 17 January 2025

Accepted: 17 January 2025

Published: 30 January 2025

Citation: Cen, Z.; Chen, Z.; Wang, D.; Zuo, Y.; Chen, X.; Chen, J. *In Vitro Investigation of Antiaging Efficacy of Pterostilbene as Cosmetic Ingredient*. *Cosmetics* **2025**, *12*, 23. <https://doi.org/10.3390/cosmetics12010023>

Copyright: © 2025 by the authors. Licensee MDPI, Basel, Switzerland. This article is an open access article distributed under the terms and conditions of the Creative Commons Attribution (CC BY) license (<https://creativecommons.org/licenses/by/4.0/>).

1. Introduction

Aging is associated with decreased physical activity, cognitive function, psychological and physical health, and resilience to stress [1]. “Antiaging” strategies aim to slow and prevent aging and extend the healthy life span [2]. Du et al. reviewed six important antiaging signal pathways: the mechanistic target of rapamycin (mTOR), AMP-activated protein kinase (AMPK), nutrient signal pathway, silent information regulator factor 2-related enzyme 1 (SIRT1), regulation of telomere length and glycogen synthase kinase-3 (GSK-3), and energy metabolism pathway, as well as their corresponding representative antiaging drugs, namely, rapamycin, metformin, acarbose, nicotinamide adenine dinucleotide (NAD⁺), lithium, and nonsteroidal anti-inflammatory drugs (NASIDS) [3]. Mishra et al. proposed antiaging therapeutic strategies. These include anti-inflammation (such as mycosporine-2-glycine, M2G), antioxidation (such as apigenin, quercetin, kaempferol, naringenin, catechins, epigallocatechin, genistein, cyanidin, resveratrol), telomere reactivation (such as 08AGTLF

from *Centella asiatica*, Nutrient 4 from *Astragalus*, TA-65 from *Astragalus membranaceus*, OA from oleanolic acid, and MA from maslinic acid), epigenetic drugs (such as spermidine and resveratrol), chaperon and proteolytic system activation (such as Btn2p, a component of the yeast anti-prion system), mitophagy activation (such as resveratrol), mTOR and insulin/IGF-1 signaling (IIS) inhibition (such as hypo-taurine), AMPK and sirtuin signaling activation (such as FDA-approved drugs biguanides, thiazolidinediones, glucagon-like peptide-1 receptor agonists, salicylates and resveratrol, 5-aminoimidazole-4-carboxamide riboside (AICAR) resveratrol and metformin, which are AMPK activators, as well as resveratrol, SRT1720, thiazolopyridine, benzimidazole, bridged ureas, cilostazol, paeonol, statins, hydrogen sulfide, persimmon, and SRT2104, which are SIRT1 activators), senescent cell clearance (such as azithromycin, roxithromycin, and curcumin), stem cell-based therapies, and microbiome regulation, among others. These strategies target nine aging hallmarks: genomic instability, telomere attrition, epigenetic alterations, loss of proteostasis, deregulated nutrient sensing, mitochondrial dysfunction, cellular senescence, stem cell exhaustion, and altered intercellular communication [4]. Liu classified antiaging substances into natural products (such as astaxanthin, curcumin, morphine, nordihydroguaiaretic acid, rapamucin, resveratrol, sappanone A, spermidine, tumbulin, urolithins, ursolic acid, coenzyme Q10, vitamins A and E, quercetin, caffeic acid, rosmarinic acid, genistein, EGCG, protandim, chicoric acid, tyrosol, fisetin, TA-65, procyanidins), endogenous substances (such as alpha-ketoglutarate, oxaloacetic acid, dehydroepiandrosterone (DHEA), 17 α -estradiol, S-Linolenoyl glutathione, melatonin, nicotinamide adenine dinucleotide (NAD⁺), nicotinamide riboside (NR), and nicotinamide mononucleotide (NMN)), drugs (such as acarbose, aspirin, (-)deprenyl, metformin, minocycline, simvastatin, celecoxib, doxycycline, enalapril, metoprolol and nebivolol), synthetic compounds (such as nitrons (4-hydroxy phenyl N-tert-butylnitron, CPI-1429), and pyridopyrimidine derivatives (compound 3a)) [5]. Significant research efforts on antiaging research are ongoing.

Pterostilbene (trans-3,5-dimethoxy-4-hydroxystilbene) is a polyphenolic compound that is naturally synthesized in some plants, such as blueberries, grapes, and pterocarpus marsupium. Pterostilbene has been reported to possess increased bioavailability and pharmacological potency over resveratrol, from which it is derived [6–8]. Pterostilbene has been extensively investigated for its beneficial biomedical applications and is expected to exert a positive effect on aging and longevity [4–9]. Pterostilbene was reported to improve obesity, liver fat, plasma cholesterol, adiposity, inflammatory biomarkers, blood glucose, and other physiological characteristics of metabolic disease in *in vitro* and *in vivo* animal models [10–12]. Furthermore, pterostilbene has been explored as an attractive drug candidate for the treatment of diseases such as diabetes, cancer, cardiovascular disease, and neurodegenerative disorders [13].

The skin is the largest organ that interfaces with the environment and plays a vital role in protecting the body from various external factors. The deterioration of skin morphology and physiology is the first and earliest obvious sign of aging [14]. Clinical research revealed that sun exposure, especially UV exposure, is responsible for 80% of visible facial aging signs [15]. Of the UV lights, UVC (100–280 nm) is completely absorbed by the ozone and does not reach the Earth's surface. UVB (280–315 nm) accounts for approximately 6% of all UV lights that reaches the Earth's surface. It is predominately absorbed by the skin's epidermis, causing DNA damage, sunburn, and other effects. UVA (315–400 nm) is lower in energy than UVB but approximately 20 times more abundant in the Earth's surface. It penetrates deeper into the dermis and is a major cause of wrinkles and roughness of the skin [16]. Thus, the development of antiaging cosmetics with UV protection activity is important for slowing the skin's aging.

The introduction of pterostilbene in skincare and cosmetics has attracted increasing attention in recent years. Pterostilbene was reported to exert skin care effects such as antioxidation, antiinflammation, whitening, enhancing cell autophagy, protection against UV damage, prevention and treatment of skin diseases *in vitro* [14,17–22], whitening, sun protection, and cure of UV-induced skin carcinoma *in vivo* [22–24]. Mechanism investigations revealed that pterostilbene realized its whitening effects by inhibiting melanogenesis, melanocyte dendritic development, and melanosome transport, which are mainly regulated by inhibiting the cAMP/PKA/CREB signal pathway [17], and protection against UVB irradiation damage through the phosphatidylinositol-3-kinase-dependent Nrf2/ARE pathway [21].

In this study, the widely used human dermal fibroblasts [25] and *in vitro* skin tissue [26] were adopted to investigate the antiaging activity of pterostilbene. UVA-irradiated fibroblasts were used to analyze the effects of pterostilbene on the expression of *collagen III*, *MMP-1*, *MMP-9*, *elastase* and *decorin* genes, as well as the content of collagen I, elastin, MMP-1, and MMP-3. UVA- and UVB-irradiated *in vitro* skin tissue was used to investigate the impact of pterostilbene on skin morphology and collagen fiber, collagen IV, collagen VII, and FGF- β content.

2. Materials and Methods

2.1. Chemicals and Reagents

The following reagents were procured and used: pterostilbene powder (A17373L01519) from Jiangsu Fengwu Biopharmaceutical Technology Co., Ltd., Nanjing, China, DMEM culture medium and nuclease-free water from Gibco, Thermo Fisher, Shanghai, China, newborn calf serum from Thermo Fisher, Shanghai, China, *in vitro* skin tissue culture medium from Boxi Biology, Guangzhou, China, dimethyl sulfoxide (DMSO), MTT, vitamin C (VC), vitamin E (VE), collagen VII antibody, and Masson staining kit from Sigma, Merck, Shanghai, China, PBS from Solibo, Beijing, China, RNAiso Plus from Accurate Biology, Changsha, China, chloroform, isopropyl alcohol, ethanol, hematoxylin, and eosin from Biyuntian, Shanghai, China, reverse transcription kit (Evo M-MLV) and fluorescent dye from Accurate Biology, Changsha, China, TGF- β 1 from Peprotech, Thermo Fisher, China, collagen I ELISA kit from Cusabio, Wuhan, China, MMP-1 ELISA kit, MMP-3 ELISA kit, elastin ELISA kit, and FGF- β ELISA Kit from Abcam, Shanghai, China, paraformaldehyde from Biosharp, Hefei, China, collagen IV antibody from Proteintech, Wuhan, China.

2.2. Fibroblast Cytotoxicity Assay

Human-originated P2 generation primary fibroblast cells (batch No. Fb19052002, Guangdong Biocell Biotechnology Co., Ltd., Dongguan, China) with proliferation capability and cell viability checked were transferred in 96-well plates at a density of 8×10^3 cells in 200 μ L of DMEM culture medium containing 10% newborn calf serum per well and cultured in a CO₂ incubator (150I, Thermo, Shanghai, China) at 37 °C with 5% CO₂ overnight until achieved 40–60% of confluence rate, which provides enough space for the cells to proliferate and enough cells for related analysis. Pterostilbene of 5.0 mg was dissolved in 1.92 mL DMSO (which was 2.6 mg/mL stock), diluted using culture medium, and added to fibroblast wells at 200 μ L per well and three wells per treatment. A solvent control (1% DMSO) and a toxicity positive control (10% DMSO) were included. After 48 h of incubation, 0.5 mg/mL of MTT was added and incubated for 4 h in dark conditions, and the OD value at 490 nm was read using a microplate reader (BioTek, Epoch, Shanghai, China). The relative cell viability was calculated as $\frac{\text{sample well OD} - \text{zero group well OD}}{\text{solvent control well OD} - \text{zero group well OD}} \times 100\%$.

2.3. Antiaging Activity Analysis Using UVA-Irradiated Fibroblasts

UVA-irradiated fibroblasts were used to investigate the antiaging efficacy of pterostilbene. Fibroblast cells cultured using DMEM culture medium were seeded into a 6-well plate at a cell density of 2×10^5 cells/well and incubated overnight at 37 °C with 5% CO₂ to reach 40–60% of confluence. The cells were then treated with 2 mL of 2.6 µg/mL pterostilbene per well and three wells per treatment for 24 h at 37 °C with 5% CO₂. After activating the UVA irradiation machine (Philips, Shanghai, China) and allowing it to run for 10 min, the cell culture solutions were replaced with 2 mL of PBS. The cell culture plates were then positioned within the UVA irradiation zone. Radiometers (PMA2110, Philips, Shanghai, China) were positioned at various points on the plates to measure the irradiation intensity (mW/cm²). The irradiation intensity was calculated as the product of the average irradiation intensity and the irradiation time. Reported studies [14] and our preliminary experiments revealed that varying doses of UVA treatment influenced fibroblast morphology and subsequent analysis endpoints. Fibroblasts demonstrated a sensitive and stable response to a dosage of around 30 J/cm² UVA irradiation [16]. Based on these findings, fibroblasts were exposed to 30 J/cm² UVA irradiation (Philips). After irradiation, the PBS solution was changed to corresponding treatment solutions and the fibroblasts were incubated at 37 °C with 5% CO₂ for 24 h. Negative (normal fibroblasts), model (UVA-irradiated only), and positive (100 ng/mL TGF-β1) controls were included. The fibroblasts were then collected for qRT-PCR analysis of the expression of aging-related genes, and the culture medium supernatant was processed for an ELISA assay of aging-related enzymes and proteins.

2.3.1. qRT-PCR Analysis

mRNA extraction: The fibroblasts in each well were rinsed twice with 1 mL of PBS and subsequently lysed with 1 mL of RNAiso Plus. The lysate was mixed thoroughly with 200 µL of chloroform by vigorous shaking (25 times), incubated at room temperature for 5 min, and centrifuged at 12,000 rpm at 4 °C for 15 min. A 400 µL aliquot of the supernatant was transferred to a new tube and combined with 400 µL of isopropanol. The mixture was shaken gently, incubated at room temperature for 5 min, and centrifuged at 12,000 rpm at 4 °C for 5 min. The resulting pellet was washed with 75% ethanol (prepared with nuclease-free water), followed by centrifugation at 12,000 rpm at 4 °C for 5 min. After air-drying the pellet in a fume hood for 10 min, it was dissolved in nuclease-free water. The concentration and quality of the extracted mRNA were assessed using a NanoDrop spectrophotometer (Thermo Fisher, Shanghai, China).

cDNA synthesis: A total mRNA of 1 µg of mRNA was combined with 2 µL of gDNA Clean Reaction Mix Ver. 2 and nuclease-free water to a final volume of 16 µL. The mixture was incubated at 42 °C for 2 min and then cooled to 4 °C. Next, 4 µL of 5× PrimeScript PR Master Mix was added, and the reaction was incubated at 37 °C for 15 min, followed by 85 °C for 5 s, and then cooled to 4 °C. The synthesized cDNA samples were stored at −20 °C for further use.

qRT-PCR: Fluorescence quantitative PCR analysis was performed using a BioRad CFX-96. Each reaction well contained a reaction mixture composed of 2 µL of cDNA, 10 µL of SYBR Green Premix Ex Taq II, 0.8 µL each of forward and reverse primers (100 µM), and nuclease-free water to a final volume of 20 µL. The qPCR protocol included an initial denaturation step at 95 °C for 30 s, followed by 40 cycles of 95 °C for 5 s and 60 °C for 30 s. A final step was performed at 67.5 °C for 5 s and 95 °C for 5 s. The primer sequences are listed in Table 1. The results were calculated using the $2^{-\Delta\Delta CT}$ method.

Table 1. Primer sequences for qRT-PCR.

Name of the Gene	Primer Sequences
<i>Collagen III</i>	F: 5'-ACCAGGAGCTAACGGTCTCA-3' R: 5'-TCTGATCCAGGGTTTCCATC-3'
<i>MMP-1</i>	F: 5'-AAGGTGGACCAACAATTTTCAGA-3' R: 5'-TGAAGGTGTAGCTAGGGTACATCAA-3'
<i>MMP-9</i>	F: 5'-CAGTCCACCCTTGTGCTCTT-3' R: 5'-ATTTTCGACTCTCCACGCATC-3'
<i>Elastase</i>	F: 5'-CGGCTACGACCCCGTAAAC-3' R: 5'-CCTGCACGTTGGCGTTGATG-3'
<i>Decorin</i>	F: 5'-GTGTGCTTGACAGTGTCTAGTG-3' R: 5'-AGTTCTGCTTGACATTCCTCCA-3'
β -Actin	F: 5'-CTGTTCCAGCCCTCCTTCAT-3' R: 5'-CCTGATGTCAATGTCGCACTTC-3'

2.3.2. ELISA Assay

The cell culture supernatant of each treatment was collected to perform the ELISA assay using MMP-1, MMP-3, collagen I, and elastin ELISA kits according to their user manuals.

2.4. Antiaging Activity Analysis Using UVA- and UVB-Irradiated *In Vitro* Skin Tissue

The *in vitro* skin tissue EpiKutis was acquired from Guangdong Biocell Biotech Co. Ltd. (Dongguan, China). Skin tissue blocks of (24 ± 2) mm² were cultured using *in vitro* skin tissue culture medium at 37 °C with 5% CO₂ for 2 days. The culture medium was changed daily. The *in vitro* skin tissues exposed to 2.6 µg/mL pterostilbene were processed for 30 J/cm² UVA and 50 mJ/cm² UVB (Philips) irradiation treatment for 4 consecutive days. After each irradiation, the culture medium was changed. The *in vitro* skin tissues were further cultured for 3 days. Negative (normal skin), model (UV-irradiated skin), and positive (100 µg/mL VC and 7 µg/mL VE) controls were included. At the end of the exposure, the treated skin tissues were processed for H&E, Masson, and immunofluorescence stains, and the culture supernatant was collected for ELISA analysis.

2.4.1. H&E Staining

H&E staining was performed to analyze the morphology of the skin tissues. Briefly, the skin tissues were fixed using 4% paraformaldehyde, embedded in paraffin wax, and sectioned. The sections were H&E-stained, photographed with an orthography microscope (Olympus, BX53, Tokyo, Japan), and analyzed with Image-Pro® Plus 6.0 image processing software.

2.4.2. Masson Staining

The skin tissue sections were stained following the Masson staining kit manual instructions. The distribution pattern and relative content of collagen fibers in the sections were photographed with an orthography microscope (Olympus, BX53, Tokyo, Japan) and analyzed with Image-Pro® Plus image processing software.

2.4.3. Immunofluorescence Staining

The distribution pattern and relative content of collagen IV and collagen VII in the skin tissue sections were analyzed with immunofluorescence staining using collagen IV and collagen VII antibodies, photographed under a fluorescence microscope (Leica, DM2500, Shanghai, China), and the integrated optical density (IOD) of the fluorescence signal was measured using Image-Pro® Plus image processing software.

2.4.4. ELISA Assay

The skin tissue culture supernatant was processed to measure the FGF- β content following the ELISA kits' manual instructions.

2.5. Statistical Analysis

Microsoft Excel (version 2410) was used to analyze the data; the results are expressed as the mean \pm SEM. The comparisons between groups were performed using a two-tailed *t*-test, and $p < 0.05$ was considered a significant difference.

3. Results

3.1. Cytotoxicity of Pterostilbene to Fibroblasts

The fibroblast cytotoxicity analysis aimed to identify the safety range of pterostilbene. Compared with the solvent control, the fibroblasts treated with 10% DMSO (toxicity positive control) proliferated poorly, and the relative cell viability was found to be $0.59\% \pm 0.30\%$ ($p < 0.001$), indicating that the fibroblasts responded normally to toxicity treatment. Based on the cell morphology (Figure 1A) and cell viability results (Figure 1B), pterostilbene at concentrations of $3.90 \mu\text{g/mL}$ or lower showed no significant toxicity to fibroblasts compared to the 1% DMSO solvent control ($p > 0.05$). However, at concentrations of 7.80 and $15.70 \mu\text{g/mL}$, pterostilbene did not alter the fibroblasts cell shape but notably reduced cell confluence and significantly ($p < 0.05$) decreased cell viability.

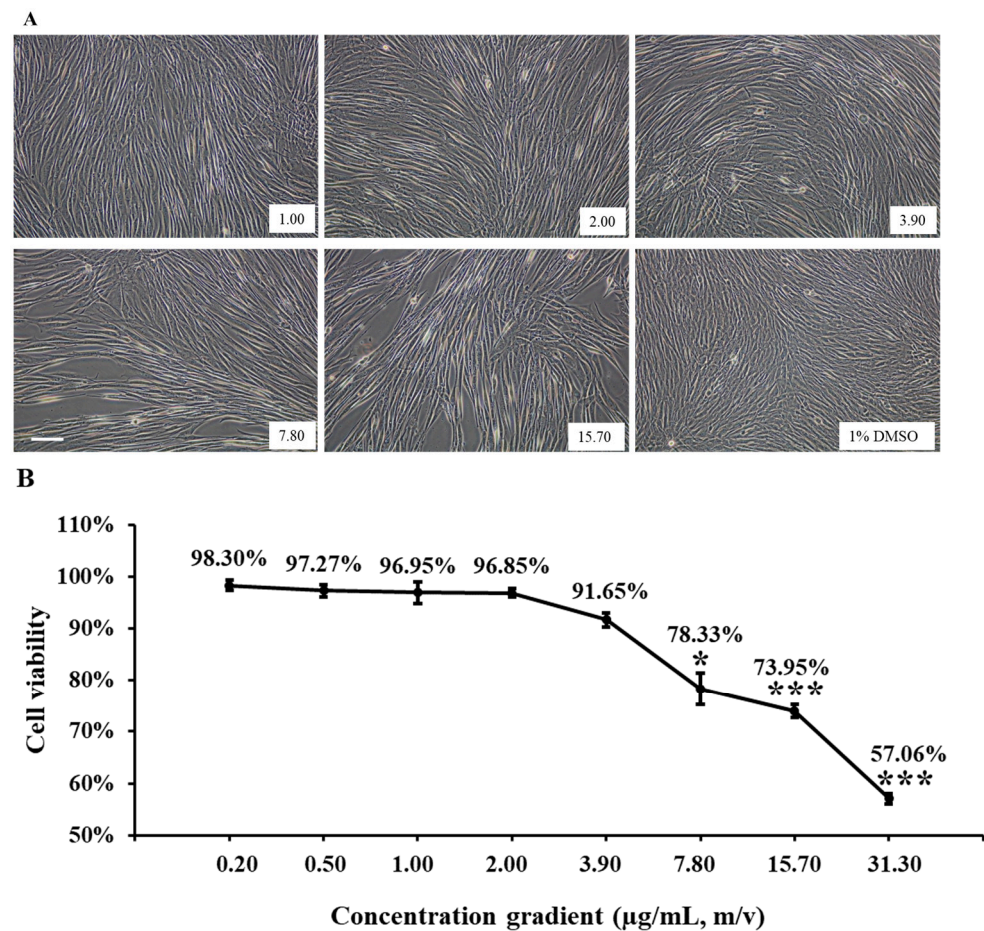


Figure 1. Cytotoxicity of pterostilbene to fibroblasts. Fibroblasts treated for 48 h were analyzed for cell viability using MTT method. (A) Fibroblast morphology. (B) Fibroblast relative viability. The scale bar equals $100 \mu\text{m}$. Data are denoted as percentage difference (mean \pm SEM) over the solvent control. Compared with the solvent control, * $p < 0.05$ and *** $p < 0.001$.

3.2. Pterostilbene Protected Fibroblasts Against UVA Irradiation

3.2.1. Pterostilbene Down-Regulated MMP-1 Gene Expression in Fibroblasts Induced by UVA Irradiation

The qRT-PCR results (Figure 2) showed that, compared with the negative control, the UVA irradiation treatment significantly up-regulated the expression of the genes *MMP-1* from 1.00 ± 0.08 to 1.88 ± 0.13 ($p = 0.001$), *MMP-9* from 1.00 ± 0.13 to 2.48 ± 0.05 ($p < 0.001$), and *elastase* from 1.00 ± 0.10 to 1.79 ± 0.27 ($p = 0.008$), but down-regulated the expression of the genes *collagen III* from 1.00 ± 0.03 to 0.64 ± 0.10 ($p = 0.04$) and *decorin* from 1.00 ± 0.03 to 0.66 ± 0.04 ($p < 0.001$) in fibroblasts.

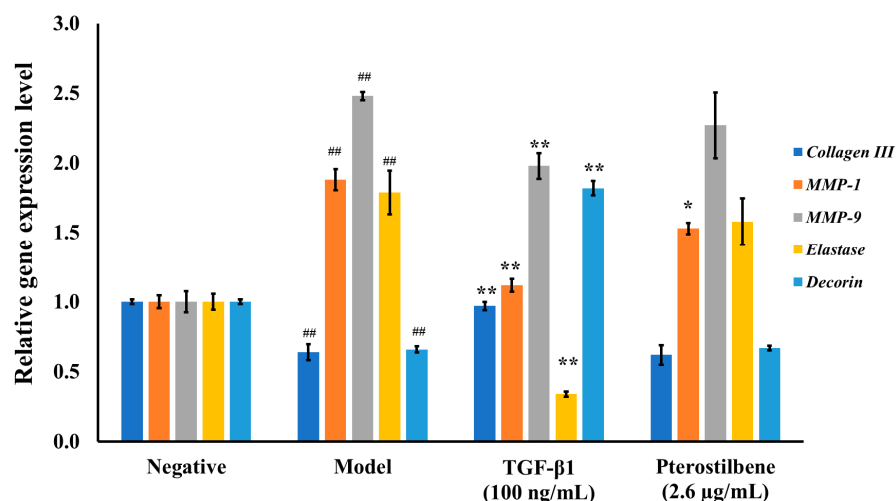


Figure 2. Pterostilbene suppressed *MMP-1* gene expression in fibroblast cells stimulated with UVA irradiation. The data are presented as mean \pm SEM of three independent experiments. Statistical significance was considered as ## $p < 0.01$ compared to the negative control and * $p < 0.05$ and ** $p < 0.01$ compared to the model control.

The TGF- β 1 (100 ng/mL) treatment that served as a positive control in this experiment showed that, compared with the UVA-irradiated model control, it significantly down-regulated the expression of the genes *MMP-1* to 1.12 ± 0.08 ($p = 0.001$), *MMP-9* to 1.98 ± 0.16 ($p = 0.007$), and *elastase* to 0.34 ± 0.03 with a decrease of ($p = 0.001$), and up-regulated the expression of the genes *collagen III* to 0.97 ± 0.05 ($p = 0.007$) and *decorin* to 1.82 ± 0.09 ($p < 0.001$), indicating its protective activity against UVA damage to fibroblasts.

The pterostilbene (2.6 μ g/mL) treatment, compared with the model control, significantly down-regulated the expression of the gene *MMP-1* to 1.53 ± 0.07 with a decrease of 18.62% ($p = 0.016$), but did not significantly ($p > 0.05$) affect the expression of the genes *MMP-9*, *elastase*, *collagen III*, and *decorin*.

3.2.2. Pterostilbene Down-Regulated MMP-1 and MMP-3 Content and Up-Regulated Collagen I Content in UVA-Radiated Fibroblasts

The ELISA analysis results (Figure 3) of the fibroblast culture supernatant revealed that, compared with the negative control, UVA irradiation (model control) significantly decreased the content of collagen I from 40.30 ± 2.26 to 30.75 ± 1.71 ($p = 0.004$) and elastin from 651.49 ± 21.75 to 266.24 ± 27.42 ($p < 0.001$), but increased the content of MMP-1 from 15.00 ± 0.67 to 85.60 ± 2.33 ($p < 0.001$) and MMP-3 from 5.97 ± 0.28 to 13.57 ± 0.26 ($p < 0.001$).

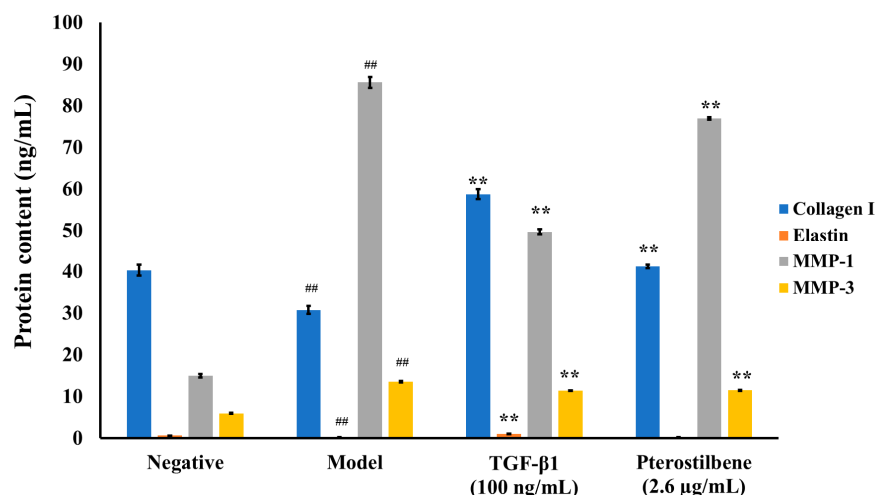


Figure 3. Pterostilbene increased collagen I content and decreased MMP-1 and MMP-3 content in fibroblast cells damaged by UVA irradiation. Model: UVA (30 J/cm²) irradiation. The data are presented as mean \pm SD of three independent experiments. Statistical significance was considered as ^{##} $p < 0.01$ compared to negative control and ^{**} $p < 0.01$ compared to model control.

The positive control TGF- β 1 (100 ng/mL) treatment, compared with the model control, significantly increased the content of collagen I to 58.76 ± 2.01 ($p < 0.001$) and elastin content to 1085.74 ± 18.47 ($p < 0.001$), but decreased the content of MMP-1 to 49.72 ± 1.12 ($p < 0.001$) and MMP-3 to 11.40 ± 0.12 ($p < 0.001$), further demonstrating its UVA protection and antiaging efficacy.

The pterostilbene (2.6 μ g/mL) treatment, compared with the model control, significantly increased collagen I content to 41.18 ± 0.68 with an increase rate of 33.92% ($p = 0.001$), however, it decreased MMP-1 and MMP-3 content to 76.98 ± 0.50 with a decrease rate of 10.08% ($p = 0.003$) and to 11.50 ± 0.223 with a decrease rate of 15.10% ($p = 0.001$), respectively, with no obvious ($p > 0.05$) effect detected for elastin. The decrease in MMP-1 and the lack of effect on elastin further confirmed the qRT-PCR results, i.e., down-regulation of *MMP-1* gene expression and no change in *elastase* gene expression by pterostilbene.

3.3. Pterostilbene Protected In Vitro Skin Against UVA and UVB Irradiation

3.3.1. Pterostilbene Maintained the Morphology of Skin Against UVA and UVB Irradiation

The H&E staining results (Figure 4) showed that, compared with normal skin (negative control), UVA and UVB irradiation-treated skin (model) showed a thinner epidermis in H&E staining, indicating that UV irradiation resulted in the loss of the extracellular matrix. The positive control VC (100 μ g/mL) and VE (7 μ g/mL) treatment, compared with the model control, obviously improved the epidermal thickness, indicating the anti-aging effects of VC and VE combination. The pterostilbene (2.6 μ g/mL)-treated skin showed similar effects to the positive control, i.e., improved thickness of the skin epidermis. These results demonstrated the antiaging effects of pterostilbene in the skin through its protection of the epidermis against UV damage.

3.3.2. Pterostilbene Protected the Collagen Fibers of Skin Against UVA and UVB Irradiation

The Masson staining results (Figure 5) revealed that, compared with normal skin (negative control), UVA- and UVB-irradiated skin (model) caused collagen fibers from 1.00 ± 0.05 to 0.35 ± 0.05 ($p < 0.001$), indicating that UV irradiation damaged collagen fibers.

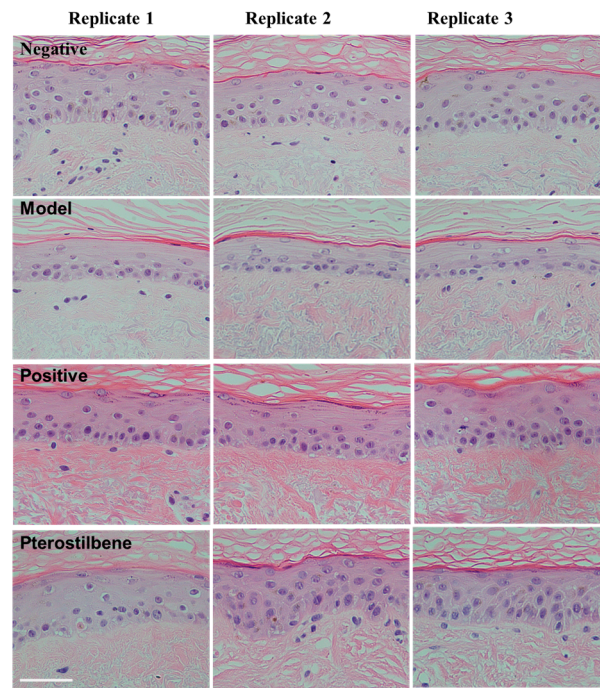


Figure 4. Pterostilbene maintained the morphology of in vitro skin against UV irradiation. Model: UVA (30 J/cm^2) + UVB (50 mJ/cm^2) irradiation for 4 consecutive days, followed by incubation for 3 days. Positive: VC ($100 \text{ }\mu\text{g/mL}$) + VE ($7 \text{ }\mu\text{g/mL}$). Scale bar equals $50 \text{ }\mu\text{m}$.

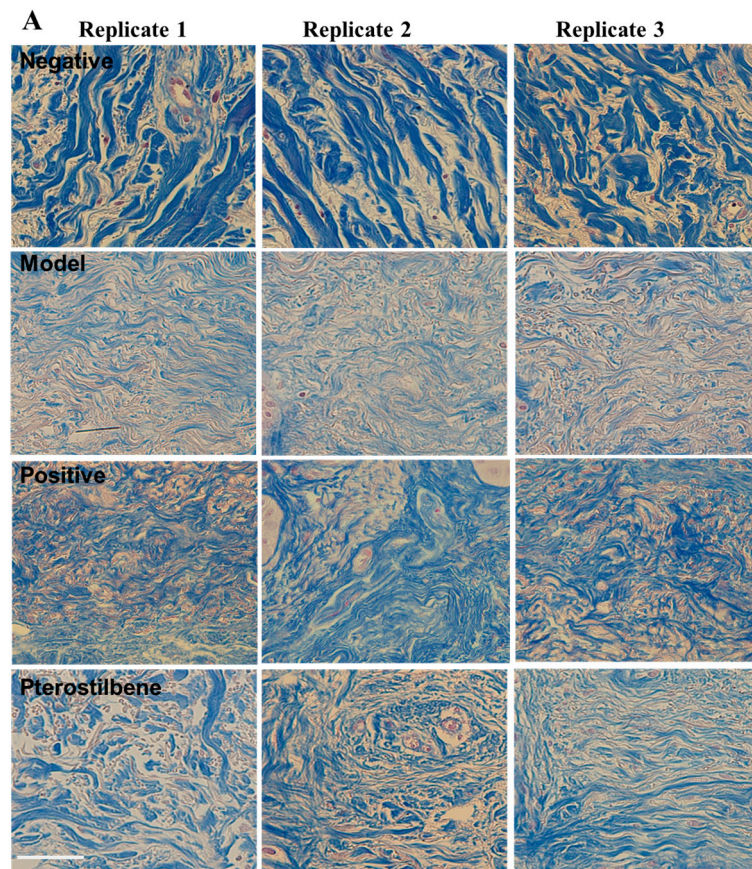


Figure 5. *Cont.*

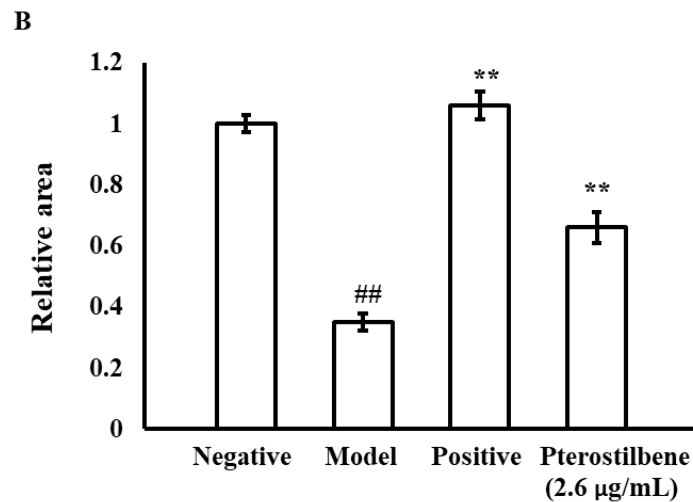


Figure 5. Pterostilbene protected the collagen fibers of in vitro skin against UV irradiation. A: The pattern (A) and content (B) of collagen fibers in skin tissues after different treatments. Model: UVA (30 J/cm²) + UVB (50 mJ/cm²) irradiation. Positive: VC (100 µg/mL) + VE (7 µg/mL). Scale bar equals 50 µm. The data are presented as mean ± SD. Statistical significance was considered as ### $p < 0.01$ compared to negative control and ** $p < 0.01$ compared to model control.

The positive control group treated with VC (100 µg/mL) + VE (7 µg/mL), compared with the model control group, showed a significant increase in collagen fiber content to 1.06 ± 0.08 , representing a 203% increase ($p < 0.001$) in the skin. These results revealed the anti-aging activity of VC + VE on the skin through its protecting collagen fibers against UV damage.

The pterostilbene (2.6 µg/mL) treatment group, compared with the model control, increased collagen fiber content to 0.66 ± 0.09 with an increase rate of 88.57% ($p = 0.005$), which demonstrated the anti-aging activity of pterostilbene on the skin through its protection of collagen fibers against UV damage.

3.3.3. Pterostilbene Increased the Content of Collagen IV, Collagen VII, and FGF-β of Skin Against UVA and UVB Irradiation

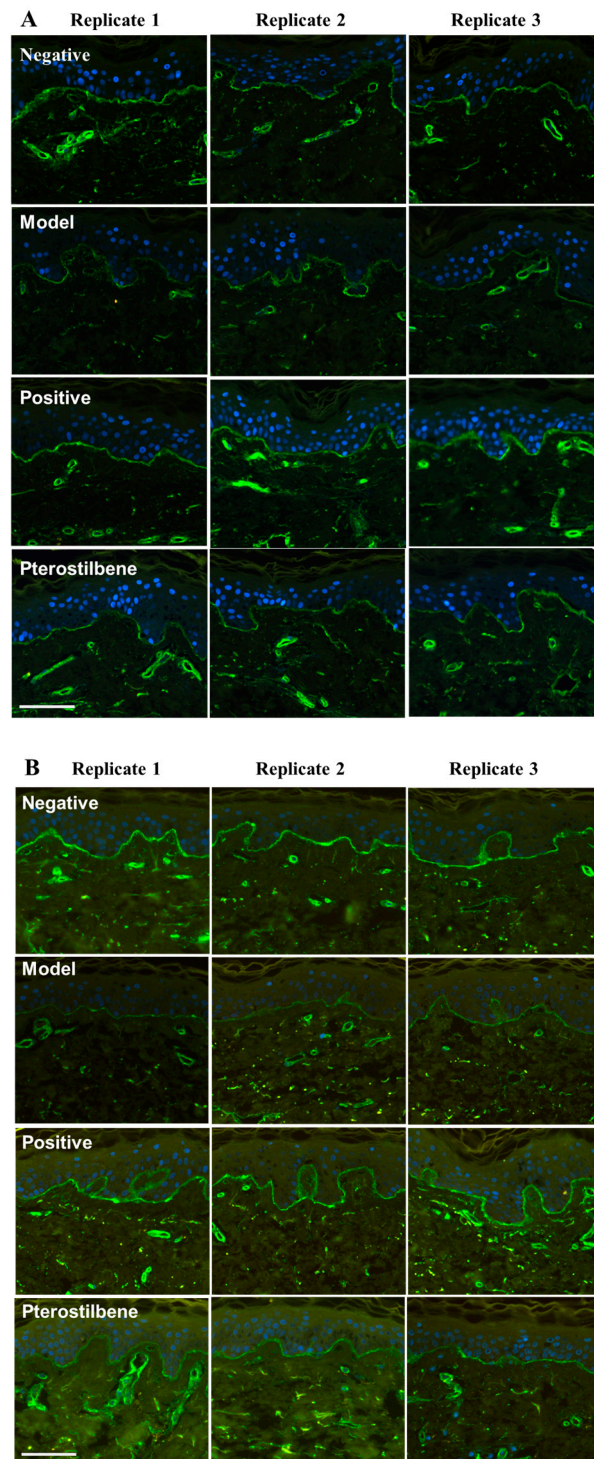
The skin sections were immunofluorescence stained to investigate the distribution pattern of collagen IV (Figure 6A) and collagen VII (Figure 6B) in the skin, and their relative content was measured and presented in Figure 6C. Additionally, the tissue culture supernatant was subjected to an ELISA assay to determine the content of FGF-β, with the results shown in Figure 6D.

The results revealed that, compared with the negative control, the model group with UV irradiation reduced the fluorescence signal of collagen IV from 1.00 ± 0.20 to 0.42 ± 0.02 ($p = 0.008$) and collagen VII from 1.00 ± 0.05 to 0.39 ± 0.05 ($p < 0.001$) in the skin, corresponding to reductions of 58% and 61%, respectively. Furthermore, UV exposure decreased the content of FGF-β in the culture supernatant from 78.45 ± 1.41 to 67.95 ± 1.29 ($p = 0.001$).

The positive control group treated with VC (100 µg/mL) + VE (7 µg/mL), compared with the model control group, improved the content of collagen IV to 0.72 ± 0.11 ($p = 0.009$) and collagen VII to 0.49 ± 0.01 ($p = 0.037$) in the skin, representing increases of 31% and 26%, respectively. Similarly, FGF-β levels in the culture medium increased to 81.82 ± 4.57 ($p = 0.007$).

The pterostilbene (2.6 µg/mL) treatment group, compared with the model control group, increased the content of collagen IV to 0.55 ± 0.07 , representing a 30.95% increase rate ($p = 0.043$), while collagen VII levels increased to 0.49 ± 0.01 , representing a 25.64% increase ($p = 0.037$). FGF-β levels in the culture medium increased to 78.60 ± 3.06 , reflecting

a 15.67% increase ($p = 0.005$). These results reflected the anti-aging activity of pterostilbene on the skin through its protection of collagen IV and collagen VII against UV damage.



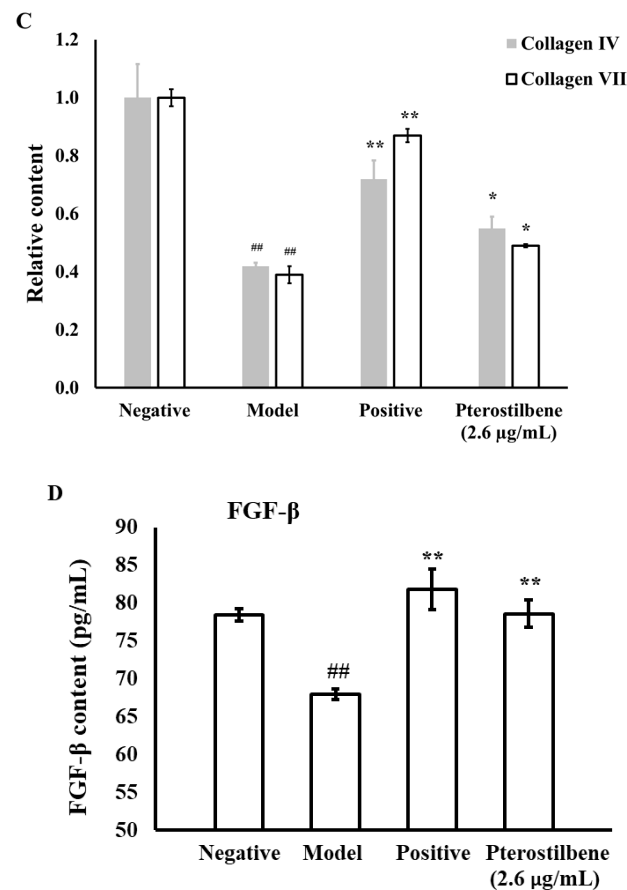


Figure 6. Pterostilbene increased collagen IV and collagen VII of in vitro skin damaged by UV irradiation. (A) The distribution pattern of collagen IV. (B) The distribution pattern of collagen VII. (C) The relative content of collagen IV and collagen VII. (D) The relative content of FGF- β . Model: UVA (30 J/cm²) and UVB (50 mJ/cm²) irradiation. Positive: VC (100 µg/mL) + VE (7 µg/mL). Scale bar equals 50 µm. The data are presented as mean \pm SD. Statistical significance was considered as ^{##} $p < 0.01$ compared to negative control, ^{*} $p < 0.05$ and ^{**} $p < 0.01$ compared to model control.

4. Discussion

The pterostilbene used in this study was a highly pure white powder (100% purity) extracted from dried *Pterocarpus marsupium* bark. It is insoluble in water but dissolves readily in most organic solvents. Pterostilbene is a natural stilbenoid and a demethylated analog of resveratrol. Both pterostilbene and resveratrol have been applied as an active ingredient in cosmetics, and resveratrol is more popular and well-known among the general public. The mechanism of regulation of resveratrol as an active ingredient in cosmetics has been investigated, and its antioxidation against UV radiation and enhanced collagen production activity have been revealed [27]. Nevertheless, the instability of resveratrol has hindered its application in skincare cosmetics, leading to the utilization of emulsification technology to improve the stability [28]. Pterostilbene, compared with resveratrol, was reported to be less toxic, more stable, and more lipophilic, and to have higher bioavailability [4–9], indicating more favorable parameters for cosmetics applications.

UV irradiation is generally recognized as the major cause of skin aging. UVB is primarily absorbed by the skin's epidermis and is the major cause of sunburns and erythema. Reports indicate that for phototype I skin, the minimal dose required to induce erythema is 20–40 mJ/cm² for UVB, compared to 20–40 J/cm² for UVA. In contrast, UVA penetrates deeper into the dermis, where it induces fibroblast apoptosis and increases collagen degradation, ultimately leading to long wrinkles and photoaging [16]. In this study, UVA irradiation was used to induce a fibroblast cell line aging model, while both UVA and UVB

were utilized to induce skin aging in vitro using the EpiKutis model. The fibroblasts assay showed that 30 J/cm² UVA irradiation enhanced the expression of the *MMP-1*, *MMP-3*, and *elastase* genes, led to an increase in MMP-1, MMP-3, and elastase enzymes, and reduced collagen I and elastin. These effects demonstrated the adverse aging effects on human dermal fibroblasts, while pterostilbene at 2.6 µg/mL alleviated the damage by suppressing *MMP-1* gene expression, decreasing MMP-1 and MMP-3 enzymes, and preventing collagen I loss. MMP-1 and MMP-3 are collagenases that hydrolyze collagen. The above data demonstrate the antiaging activity of pterostilbene against UVA radiation through its protection of collagen from degradation. Notably, both gene expression analysis and ELISA assay results showed that pterostilbene was unable to protect elastin degradation caused by UVA irradiation. The in vitro skin study results show that UVA and UVB irradiation reduced skin morphology to a thinner epidermis, degraded skin collagen fibers, and, more specifically, reduced the content of collagen IV, collagen VII, and FGF-β in the skin. Pterostilbene treatment was found to protect in vitro skin from UV irradiation damage by reducing, with varying potency, all the adverse aging effects. Thus, both the fibroblast study and the in vitro skin experiment demonstrated the antiaging efficacy of pterostilbene through its protection of skin from UV irradiation-triggered degradation stress.

Compared with the widely studied biomedical applications [6–13], pterostilbene is a much less studied ingredient for cosmetics. The present study revealed the antiaging efficacy of pterostilbene against UV irradiation in vitro. Similarly, previous research has shown that pterostilbene mitigates UV-induced damage through Nrf2-mediated antioxidant pathways. For example, it alleviated damage caused by 3 J/cm² UVA irradiation to human keratinocyte HaCaT cells at concentrations of 2.5–5 µM (0.64–1.28 µg/mL) [21], reduced damage from 300 mJ/cm² UVB irradiation to HaCaT cells at concentrations of 5–10 µM (1.28–2.56 µg/mL) [18], and attenuated damage from 20 J/cm² UVA and 57 mJ/cm² UVB irradiation to HaCaT cells at a concentration of 9.75 µM (2.5 µg/mL) [29]. Additionally, pterostilbene has been reported to protect HaCaT keratinocytes against oxidative stress, inflammation, and aging induced by 20 µM particulate matter (a major air pollutant) [25]. It also showed protective effects in hairless mice, safeguarding against acute UVB (360 mJ/cm²) irradiation and chronic UVB (180 mJ/cm², three doses/week for six months)–induced skin damage and carcinogenesis [24]. These findings underscore pterostilbene’s ability to effectively protect the skin from UV irradiation and environmental stressors. The excellent UV protection and antiaging potency identified in this paper and previous studies justify the value of adding pterostilbene into cosmetic formulations designed to combat UV and pollution-induced damage. Moreover, these results highlight the importance of further investigation into the mechanisms involved in the regulation and clinical monitoring of pterostilbene-containing cosmetics.

5. Conclusions

The present investigation examined the antiaging activity of pterostilbene using a human dermal fibroblast assay and an in vitro skin experiment. Pterostilbene at 2.6 µg/mL reduced MMP-1 by 10.08% and MMP-3 by 15.10%, increased collagen I by 33.92% in UVA-treated fibroblasts, improved tissue morphology, and up-regulated collagen fibers by 88.57%, collagen IV by 30.95%, collagen VII by 25.64%, and FGF-β by 15.67% content in UVA- and UVB-irradiated in vitro skin. All the metrics demonstrate that pterostilbene can alleviate skin UVA and UVB irradiation damage by reducing collagen degradation. These experimental results revealed the promising antiaging potency of pterostilbene as a cosmetic ingredient with multiple pathways affecting skin health.

Author Contributions: Z.C. (Zongxiao Cen) and Z.C. (Zhiyuan Chen) designed and coordinated this study and proofread the article; D.W., Y.Z. and J.C. performed and analyzed the experiments; X.C. designed, analyzed, and wrote the article. All authors have read and agreed to the published version of the manuscript.

Funding: This research received no external funding.

Institutional Review Board Statement: Not applicable.

Informed Consent Statement: Not applicable.

Data Availability Statement: Data is contained within the article.

Acknowledgments: We would like to thank Shaanxi BioCell General Testing Co., Ltd. for their technical support.

Conflicts of Interest: Authors Z.C. (Zongxiao Cen), Z.C. (Zhiyuan Chen), D.W., and Y.Z. were employed by the company Guangzhou Luanying Cosmetics Co., Ltd. Authors X.C., and J.C. were employed by the company Vitargent (International) Biotechnology Limited The authors declare that the research was conducted in the absence of any commercial or financial relationships that could be construed as a potential conflict of interest.

Abbreviations

MMP-1	matrix metalloproteinase 1
MMP-3	matrix metalloproteinase 3
MMP-9	matrix metalloproteinase 9
FGF- β	fibroblast growth factor- β
mTOR	mechanistic target of rapamycin
AMPK	AMP-activated protein kinase
SIRT1	silent information regulator factor 2-related enzyme 1
GSK-3	glycogen synthase kinase-3
NAD+	nicotinamide adenine dinucleotide
NASIDS	nonsteroidal anti-inflammatory drugs
M2G	mycosporine-2-glycine
AICAR	5-aminoimidazole-4-carboxamide riboside
DHEA	dehydroepiandrosterone
NR	nicotinamide riboside
NMN	nicotinamide mononucleotide
DMSO	dimethyl sulfoxide
VC	vitamin C
VE	vitamin E
IOD	integrated optical density
H&E staining	hematoxylin and eosin staining
Nrf2	nuclear factor erythroid 2-related factor 2

References

1. Rowe, J.W.; Kahn, R.L. Successful aging. *Gerontologist* **1997**, *37*, 433–440. [[CrossRef](#)]
2. Campisi, J.; Kapahi, P.; Lithgow, G.J.; Melov, S.; Newman, J.C.; Verdin, E. From discoveries in age-ing research to therapeutics for healthy ageing. *Nature* **2019**, *571*, 183–192. [[CrossRef](#)] [[PubMed](#)]
3. Du, N.; Yang, R.; Jiang, S.; Niu, Z.; Zhou, W.; Liu, C.; Gao, L.; Sun, Q. Anti-aging drugs and the related signal pathways. *Biomedicines* **2024**, *12*, 127. [[CrossRef](#)]
4. Mishra, S.K.; Balendra, V.; Esposto, J.; Obaid, A.A.; Maccioni, R.B.; Jha, N.K.; Perry, G.; Moustafa, M.; Al-Shehri, M.; Singh, M.P.; et al. Therapeutic antiaging strategies. *Biomedicines* **2022**, *10*, 2515. [[CrossRef](#)] [[PubMed](#)]

5. Liu, J.K. Antiaging agents: Safe interventions to slow aging and healthy life span extension. *Nat. Prod. Bioprospect.* **2022**, *12*, 18. [[CrossRef](#)]
6. Chan, E.W.C.; Wong, C.W.; Tan, Y.H.; Foo, J.P.Y.; Wong, S.K.; Chan, H.T. Resveratrol and pterostilbene: A comparative overview of their chemistry, biosynthesis, plant sources and pharmacological properties. *J. Appl. Pharm. Sci.* **2019**, *9*, 124–149.
7. Nagarajan, S.; Mohandas, S.; Ganesan, K.; Xu, B.; Ramkumar, K.M. New insights into dietary pterostilbene: Sources, metabolism, and health promotion effects. *Molecules* **2022**, *27*, 6316. [[CrossRef](#)] [[PubMed](#)]
8. Kim, H.; Seo, K.H.; Yokoyama, W. Chemistry of pterostilbene and its metabolic effects. *J. Agric. Food Chem.* **2020**, *68*, 12836–12841. [[CrossRef](#)]
9. Li, Y.R.; Li, S.; Lin, C.C. Effect of resveratrol and pterostilbene on aging and longevity. *Biofactors* **2018**, *44*, 69–82. [[CrossRef](#)] [[PubMed](#)]
10. Wang, S.; Zhou, X.; He, X.; Ma, S.; Sun, C.; Zhang, J.; Xu, X.; Jin, W.; Yan, J.; Lin, P.; et al. Suppressive effects of pterostilbene on human cytomegalovirus (HCMV) infection and HCMV-induced cellular senescence. *Viol. J.* **2022**, *19*, 224. [[CrossRef](#)]
11. Lin, W.S.; Leland, J.V.; Ho, C.T.; Pan, M.H. Occurrence, bioavailability, anti-inflammatory, and anticancer effects of pterostilbene. *J. Agric. Food Chem.* **2020**, *68*, 12788–12799. [[CrossRef](#)]
12. Dodda, D.; Ciddi, V. Pterostilbene alleviates diabetic nephropathy in experimental diabetic rats; inhibition of aldose reductase and advanced glycation end products formation. *Orient. Pharm. Exp. Med.* **2015**, *15*, 297–303. [[CrossRef](#)]
13. Gómez-Zorita, S.; Milton-Laskibar, I.; Aguirre, L.; Fernández-Quintela, A.; Xiao, J.; Portillo, M.P. Effects of pterostilbene on diabetes, liver steatosis and serum lipids. *Curr. Med. Chem.* **2021**, *28*, 238–252. [[CrossRef](#)]
14. Teng, W.L.; Huang, P.H.; Wang, H.C.; Tseng, C.-H.; Yen, F.-L. Pterostilbene attenuates particulate matter-induced oxidative stress, inflammation and aging in keratinocytes. *Antioxidants* **2021**, *10*, 1552. [[CrossRef](#)] [[PubMed](#)]
15. Flament, F.; Bazin, R.; Laquieze, S.; Rubert, V.; Simonpietri, E.; Piot, B. Effect of the sun on visible clinical signs of aging in Caucasian skin. *Clin. Cosmet. Investig. Dermatol.* **2013**, *6*, 221–232. [[CrossRef](#)] [[PubMed](#)]
16. Guan, L.L.; Lim, H.W.; Mohammad, T.F. Sunscreens and photoaging: A review of current literature. *Am. J. Clin. Dermatol.* **2021**, *22*, 819–828. [[CrossRef](#)] [[PubMed](#)]
17. An, X.; Lv, J.; Wang, F. Pterostilbene inhibits melanogenesis, melanocyte dendricity and melanosome transport through cAMP/PKA/CREB pathway. *Eur. J. Pharmacol.* **2022**, *932*, 175231. [[CrossRef](#)] [[PubMed](#)]
18. Li, H.; Jiang, N.; Liang, B.; Liu, Q.; Zhang, E.; Peng, L.; Deng, H.; Li, R.; Li, Z.; Zhu, H. Pterostilbene protects against UVB-induced photo-damage through a phosphatidylinositol-3-kinase-dependent Nrf2/ARE pathway in human keratinocytes. *Redox Rep.* **2017**, *22*, 501–507. [[CrossRef](#)] [[PubMed](#)]
19. Tang, K.W.; Hsu, C.Y.; Aljuffali, I.A.; Alalaiwe, A.; Lai, W.-N.; Gu, P.-Y.; Tseng, C.-H.; Fang, J.-Y. Skin delivery of synthetic benzoyl pterostilbenes suppresses atopic dermatitis-like inflammation through the inhibition of keratinocyte and macrophage activation. *Biomed. Pharmacother.* **2024**, *170*, 116073. [[CrossRef](#)]
20. Chen, R.-J.; Lee, Y.-H.; Yeh, Y.-L.; Wu, W.-S.; Ho, C.-T.; Li, C.-Y.; Wang, B.-J.; Wang, Y.-J. Autophagy-inducing effect of pterostilbene: A prospective therapeutic/preventive option for skin diseases. *J. Food Drug Anal.* **2017**, *25*, 125–133. [[CrossRef](#)]
21. Hseu, Y.-C.; Gowrisankar, Y.V.; Wang, L.-W.; Zhang, Y.-Z.; Chen, X.-Z.; Huang, P.-J.; Yen, H.-R.; Yang, H.-L. The *in vitro* and *in vivo* depigmenting activity of pterostilbene through induction of autophagy in melanocytes and inhibition of UVA-irradiated α -MSH in keratinocytes via Nrf2-mediated antioxidant pathways. *Redox Biol.* **2021**, *44*, 102007. [[CrossRef](#)] [[PubMed](#)]
22. Majeed, M.; Majeed, S.; Jain, R.; Mundkur, L.; Rajalakshmi, H.R.; Lad, P.; Neupane, P. A randomized study to determine the sun protection factor of natural pterostilbene from *Pterocarpus marsupium*. *Cosmetics* **2020**, *7*, 16. [[CrossRef](#)]
23. Majeed, M.; Majeed, S.; Jain, R.; Mundkur, L.; Rajalakshmi, H.R.; Lad, P.S.; Neupane, P. An open-label single-arm, monocentric study assessing the efficacy and safety of natural pterostilbene (*Pterocarpus marsupium*) for skin brightening and antiaging effects. *Clin. Cosmet. Investig. Dermatol.* **2020**, *13*, 105–116. [[CrossRef](#)] [[PubMed](#)]
24. Sirerol, J.A.; Feddi, F.; Mena, S.; Rodriguez, M.L.; Sirera, P.; Aupí, M.; Pérez, S.; Asensi, M.; Ortega, A.; Estrela, J.M. Topical treatment with Pterostilbene, a natural phytoalexin, efficiently protects hairless mice against UVB-radiation induced skin damage and carcinogenesis. *Free Radiat. Biol. Med.* **2015**, *85*, 1–11. [[CrossRef](#)] [[PubMed](#)]
25. Reynolds, W.J.; Hanson, P.S.; Critchley, A.; Griffiths, B.; Chavan, B.; Birch-Machin, M.A. Exposing human primary dermal fibroblasts to particulate matter induces changes associated with skin aging. *FASEB J.* **2020**, *34*, 14725–14735. [[CrossRef](#)] [[PubMed](#)]
26. Suhail, S.; Sardashti, N.; Jaiswal, D.; Rudraiah, S.; Misra, M.; Kumbar, S.G. Engineered skin tissue equivalents for product evaluation and therapeutic applications. *Biotechnol. J.* **2019**, *14*, e1900022. [[CrossRef](#)] [[PubMed](#)]
27. Ratz-Lyko, A.; Arct, J. Resveratrol as an active ingredient for cosmetic and dermatological applications: A review. *J. Cosmet. Laser Ther.* **2019**, *21*, 84–90. [[CrossRef](#)] [[PubMed](#)]

28. Das, S.; Lee, S.H.; Chow, P.S.; Macbeath, C. Microemulsion composed of combination of skin beneficial oils as vehicle: Development of resveratrol-loaded microemulsion based formulations for skin care applications. *Colloids Surf. B Biointerfaces* **2020**, *194*, 111161. [[CrossRef](#)] [[PubMed](#)]
29. Deng, H.; Li, H.; Ho, Z.Y.; Dai, X.Y.; Chen, Q.; Li, R.; Liang, B.; Zhu, H. Pterostilbene's protective effects against photodamage caused by UVA/UVB irradiation. *Pharmazie* **2018**, *73*, 651–658.

Disclaimer/Publisher's Note: The statements, opinions and data contained in all publications are solely those of the individual author(s) and contributor(s) and not of MDPI and/or the editor(s). MDPI and/or the editor(s) disclaim responsibility for any injury to people or property resulting from any ideas, methods, instructions or products referred to in the content.